Am. J. Hum. Genet. 57:832–839, 1995

Genetic Mapping of the Dentinogenesis Imperfecta Type II Locus

Andrew H. Crosby,[1] Titia Scherpbier-Heddema,[2] Cisca Wijmenga,[3,*] Michael R. Altherr,[4] Jeffrey C. Murray,[5] Kenneth H. Buetow,[2] and Michael J. Dixon[1]

[1]School of Biological Sciences and Departments of Dental Medicine and Surgery, University of Manchester, Manchester, England; [2]Division of Population Science, Fox Chase Cancer Center, Philadelphia; [3]MGC—Department of Human Genetics, Leiden University, Leiden; [4]Los Alamos National Laboratory, Genomics and Structural Biology, Los Alamos; and [5]Department of Pediatrics and Biological Sciences, University of Iowa Hospitals and Clinics, Iowa City

Summary

Dentinogenesis imperfecta type II (DGI-II) is an autosomal dominant disorder of dentin formation, which has previously been mapped to chromosome 4q12-21. In the current study, six novel short tandem-repeat polymorphisms (STRPs) have been isolated, five of which show significant evidence of linkage to DGI-II. To determine the order of the STRPs and define the genetic distance between them, nine loci (including polymorphisms for two known genes) were mapped through the CEPH reference pedigrees. The resulting genetic map encompasses 16.3 cM on the sex-averaged map. To combine this map with a physical map of the region, all of the STRPs were mapped through a somatic cell hybrid panel. The most likely location for the DGI-II locus within the fixed marker map is in the D4S2691–D4S2692 interval of 6.6 cM. The presence of a marker that shows no recombination with the DGI-II phenotype between the flanking markers provides an important anchor point for the creation of physical continuity across the DGI-II candidate region.

Introduction

Dentinogenesis imperfecta (DGI) is an autosomal dominant disorder of dental development, which occurs with an incidence of ~1:8,000 live births (Witkop et al. 1957). DGI disrupts dentin formation, resulting in severely discolored, translucent teeth. The enamel, although unaffected, tends to fracture, exposing the softened underlying dentin, which undergoes rapid attrition leading to a marked shortening of the teeth. The root canals become partially or totally obliterated by continued dentin formation, and the roots tend to be attenuated. Both root fractures and periapical infections are common. As a result, DGI entails protracted dental care, with extensive, frequently unpleasant treatment required. Since the disorder presents within the first few months of life, with the eruption of the primary dentition, there may be severe psychosocial consequences, associated with poor esthetic appearance, and the development of anxiety regarding dental treatment. The identification of the underlying molecular abnormality might suggest strategies for the amelioration and prevention of DGI. Investigation of the expression of this gene and its protein product during normal development—and of its interaction with other molecules—would provide insights into the fundamental mechanisms involved in normal dentinogenesis.

On the basis of genetic linkage to a protein polymorphism at the vitamin D–binding protein locus, GC, the gene mutated in isolated DGI (DGI-II) has been localized to chromosome 4q12-q21 (maximum lod score [Z_{max}] 7.9 at recombination fraction [θ] .13) (Ball et al. 1982). Subsequent segregation analysis has shown that the gene INP-10 is tightly linked to DGI-II (Z_{max} = 3.91 at θ = .00) (Crall et al. 1992). Additional linkage studies have shown that a number of other dental disorders map to this region of the genome, including Rieger syndrome (Murray et al. 1992), juvenile periodontitis (Boughman et al. 1986), and an autosomal dominant form of amelogenesis imperfecta (Forsman et al. 1994). To date, the candidate genes amphiregulin, epidermal growth factor, and dentin phosphoprotein have been excluded from a causative role in pathogenesis of DGI-II (Crall et al. 1992; MacDougall et al. 1992). In the absence of further candidate genes, the creation of a high-resolution genetic map around the DGI-II locus, as well as the identification of close flanking markers, will be central to the isolation of the mutated gene. However, relatively few highly informative polymorphic markers have been accurately positioned within this region of the genome (Mills et al. 1992; Bakker et al. 1994; Buetow et al. 1994; Gyapay et al. 1994).

In the current investigation a number of moderately to highly informative short tandem-repeat polymorphisms (STRPs) have been produced from cosmids that pre-

Received May 11, 1995; accepted for publication July 7, 1995.

Address for correspondence and reprints: Dr. Michael J. Dixon, School of Biological Sciences, 3.239, Stopford Building, University of Manchester, Manchester M13 9PT, United Kingdom.

* Present address: National Center for Genome Research, NIH, Bethesda.

0002-9297/95/5704-0013$02.00

Table 1

STRPs Isolated in the Present Study

Locus	Primer Sequences (5′–3′)	Annealing Temperature	Heterozygosity
D4S2689	TGCTGCCAGATTCAGTTTGC GTTCTGTGAGCCCAGTATTG	55°C	.78
BMP3	CAGGTCCTTGCTCCCAATGT CAGTGGGGAGGATATTTGGC	57°C	.55
D4S2690	CACTCCAGCCTGGGCAAC AGTTGCATCCTCAGAACCTC	55°C	.88
D4S2691	CGAGCCAATTGAGAGGTACT ATATGCAGGTTACTCCCAGG	55°C	.78
D4S2692	CAACGCAAGACACTGGTTGT CCAAATAGAAATCGCTCCCC	55°C	.76
D4S2693	CTTGAGAAGAACTATAGTAGCA TTGACTTTATTCCGTTAAGGAC	55°C	.51

viously have been mapped to the long arm of chromosome 4 by FISH (Wijmenga et al., in press). To create a high-resolution genetic map of the 4q21-23 region, these loci have been placed on a reference map using the CEPH pedigrees (Dausset et al. 1990). These markers have also been used to screen a somatic cell hybrid (SCH) panel (Goold et al. 1993), thereby allowing combination of the genetic and physical maps of the region. Segregation analysis within two large DGI-II families has allowed us to position the DGI-II locus within this map and to identify markers flanking the disease locus.

Material and Methods

Marker Isolation

The isolation of cosmids from the Los Alamos chromosome 4 cosmid library, as well as their mapping to chromosome 4q, have been described elsewhere (Wijmenga et al., in press). YAC clones encompassing the BMP3 locus were isolated from the ICI library (Anand et al. 1990) by a hybridization-based strategy. The isolation of STRPs from YACs and cosmids, as well as their optimization and utilization for genotyping, have been described elsewhere (Dixon et al. 1992; Crosby et al. 1995). The primers are detailed in table 1. Three additional STRPs—D4S451 (Goold et al. 1993), D4S400 (Gyapay et al. 1994), and SPP1 (Crosby et al. 1995)—were also used in the study. Negative controls were established for all reactions.

Linkage Analysis

Genotyping of all markers was carried out on the CEPH reference panel (Dausset et al. 1990). A framework map was constructed from these data, with the analysis program CRIMAP, version 2.4, by standard methods detailed by Buetow et al. (1992). In brief, with the loci D4S2689 and D4S2692 used as starting points, new loci were considered for introduction into the map, in the order of their information content. Loci with unique placements supported by odds $\geq$1,000:1 were added to the map. After no new loci could be added to the map, support for the final map was confirmed by considering the likelihood of inversions of points immediately adjacent within the map. A map-contraction diagnostic algorithm (LENLOC) was also used, in which individual loci were sequentially removed from the map, and the effect on the average length of the map was noted.

The pedigrees of the two DGI-II families used in the current study have been described elsewhere (Crall et al. 1992). The alleles were scored, and the data were coded for genetic linkage analysis. The DGI-II locus was modeled as an autosomal dominant, two-allele system. The gene frequency and the penetrance in heterozygotes were taken as .00001 and .99, respectively. Pairwise analysis was performed by the MLINK routine of the LINKAGE package (Lathrop et al. 1984). Maximum-likelihood estimates of sex-averaged recombination were calculated by ILINK. Significance was evaluated by the standard criterion (lod score [Z] > 3.0). Multipoint analysis was performed with the LINKMAP routine of the LINKAGE package (Lathrop et al. 1985). A 1-lod difference from the maximum-likelihood estimate was used to construct a support (confidence) interval (Conneally et al. 1985).

SCH Analysis

The chromosome 4 content of the hybrid cell lines used in the study is depicted in figure 1*A*. The hybrid cell lines were screened with all of the loci detailed above, by PCR. PCR assays were performed in 25-μl reaction volumes containing 20 ng genomic DNA; 50

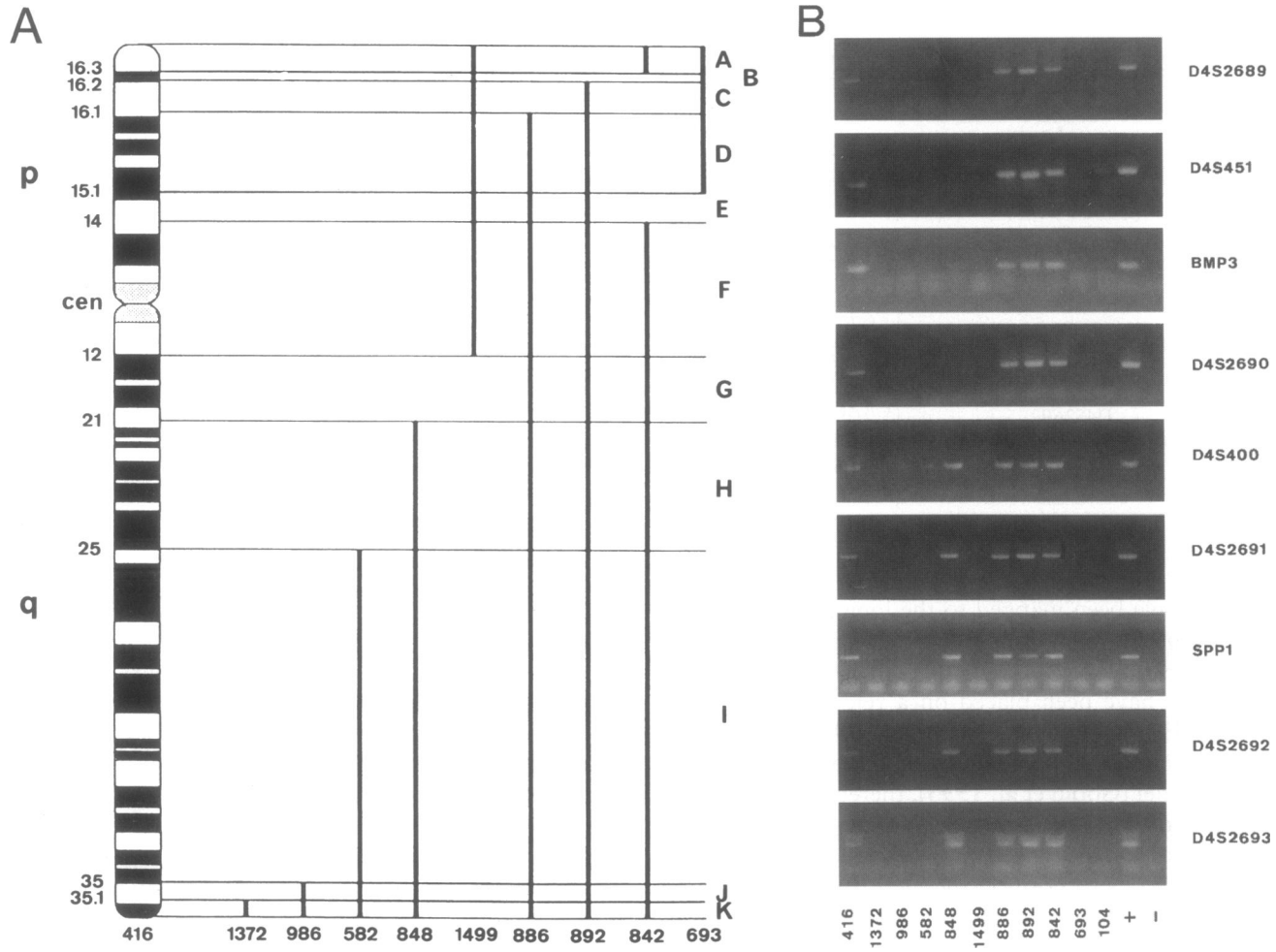

Figure 1 *A*, Ideogram depicting the chromosome 4 component of the SCHs used in the current study. *B*, PCR analysis of the 10 loci used in the current study, across the SCH panel. Cell line 104 contains hamster DNA only. D4S2689, D4S451, BMP3, and D4S2690 produce positive signals in hybrids 886, 892, and 842, indicating that they are located within region G (4q12-21), whereas D4S400, D4S2691, SPP1, D4S2692, and D4S2693 produce an additional signal in hybrid 848, indicating that they are located within region H (4q21-25).

pmol each primer; 200 μM each of dCTP, dGTP, dTTP, and dATP; 10 mM Tris-HCl pH 8.3; 50 mM KCl; 1 mM $MgCl_2$; and 0.01% gelatin. The samples were overlaid with mineral oil, heated to 96°C for 10 min, and cooled to 55°C. After addition of 0.75 U *Taq* DNA polymerase, the samples were processed through 35 amplification cycles of 92°C for 30 s, primer-annealing temperature for 30 s (table 1), and 72°C for 30 s, with a Hybaid thermal cycler. The final extension step was lengthened to 10 min. Positive (total human genomic DNA) and negative (water and hamster cell line UCW 104 DNA) controls were established for all reactions. The PCR products were analyzed on a 3% agarose gel.

Results

Previous segregation studies in DGI-II families have shown that the DGI-II locus is linked to the markers GC and INP10, which have been localized to chromosomes 4q13-21 and 4q21, respectively (Ball et al. 1982; Crall et al. 1992). Nevertheless, the DGI-II locus has not been positioned on the genetic maps of this region. Moreover, relatively few STRPs have been accurately positioned within this region of the genome (Mills et al. 1992; Bakker et al. 1994; Buetow et al. 1994; Gyapay et al. 1994). As a prelude to the creation of a high-resolution genetic map surrounding the DGI-II locus, five STRPs were isolated from cosmids that had previously been mapped to the long arm of chromosome 4 by FISH. All of the STRPs were shown to be inherited in a codominant Mendelian fashion and were moderately to highly polymorphic (table 1).

To establish their physical location, the STRPs were first used to screen an SCH panel. The chromosome 4 region retained in each hybrid cell line is indicated in figure 1*A*. The results of this analysis indicated that

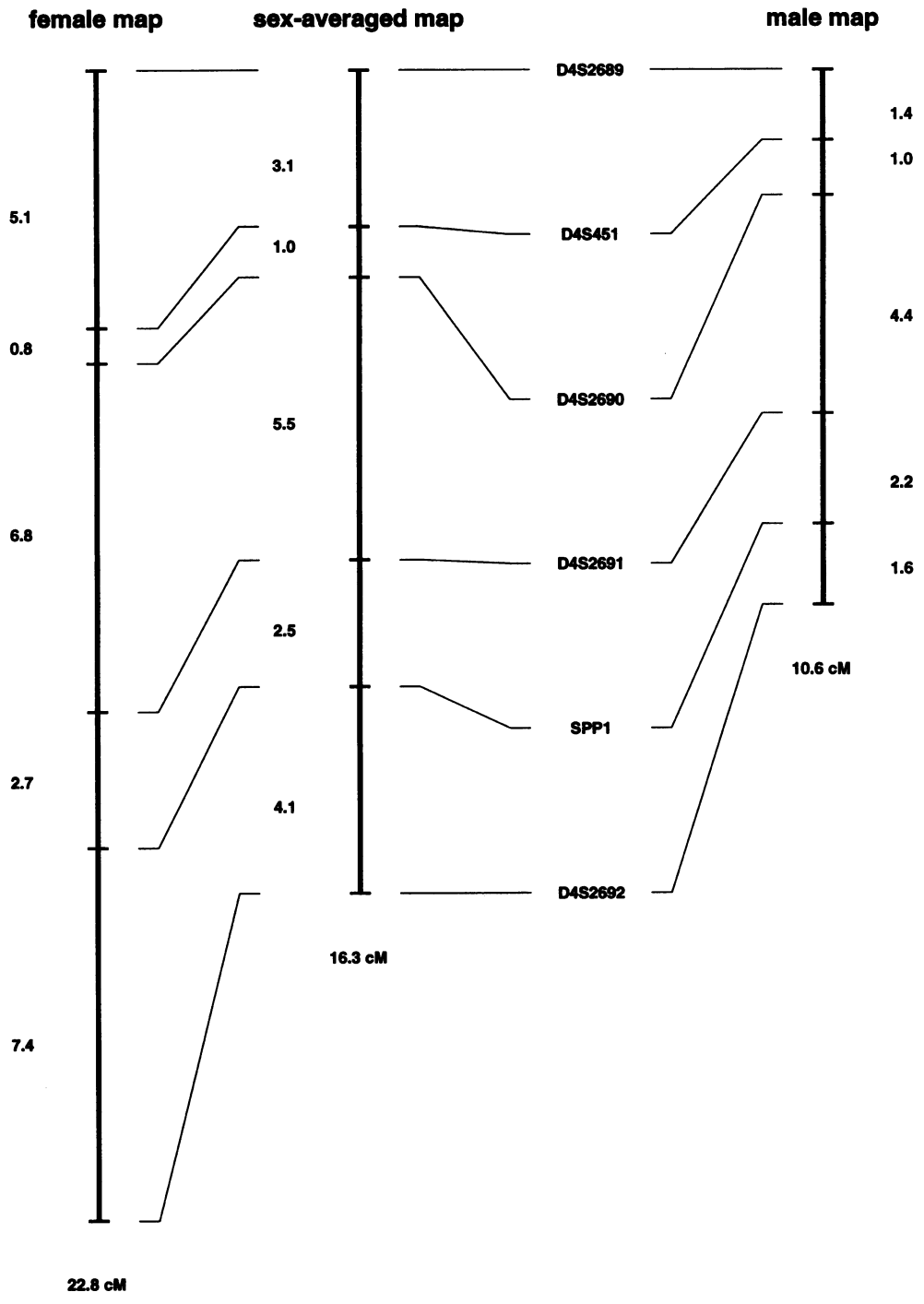

Figure 2 Sex-averaged and sex-specific framework maps of 4q12-23. All the loci are positioned with odds ≥1,000:1 against inversion of adjacent pairs, and interlocus intervals (in cM) are calculated under the assumption of Kosambi level interference.

D4S2689, D4S451, and D4S2690 are located within region G (4q12-21), whereas D4S400, D4S2691, SPP1, D4S2692, and D4S2693 are more distally located, in region H (4q21-25) (fig. 1*B*). The locations of D4S451 and SPP1 are in agreement with those reported by Goold et al. (1993). Given that the BMP3 locus has previously been mapped to 4p14-q21 (Tabas et al. 1991), PCR primers designed from BMP3 cDNA sequence (5′-TGT-AGTGCTTAAAGTATACCC-3′ and 5′-CAAATGAG-TTCTTTGCCAGG-3′) were used to screen the SCH panel. Since this analysis indicated that the BMP3 locus also lies in region G (fig. 1), a search for an STRP at

Table 2

Results of the Map-Contraction Diagnostic Algorithm

Locus	Map Location (cM)	Map Length without Locus (cM)	Change in Map Length (cM)
D4S2689	.0	...	...
D4S451	3.1	15.7	−.60
D4S2690	4.1	16.5	.20
D4S2691	9.7	16.4	.10
SPP1	12.2	15.6	−.70
D4S2692	16.3	...	...

this locus was undertaken. The BMP3 cDNA was therefore used to screen the ICI YAC library by hybridization, and a 325-kb YAC clone (24HF8) was isolated. Primers flanking an STRP isolated from this clone were also shown to map to region G (data not shown).

To define the genetic distance between the isolated STRPs and to extend the resulting genetic map to include additional markers from this region, nine loci, including two known genes, were mapped through the CEPH panel. Six of these loci, including SPP1, were positioned on the map with odds ≥1,000:1 (fig. 2). The resulting sex-averaged map covers 16.3 cM (the female map extends over 22.8 cM, and the male map extends over 10.6 cM) (fig. 2). The results generated with the map-contraction diagnostic algorithm are presented in table 2. These results indicate that the removal of any individual locus has little effect on the total map length, providing additional support for the accuracy of the map. Of the loci that could not be positioned on the genetic map with lod-3 support, the most likely location for D4S400 is in the interval between D4S2690 and D4S2691 (lod 2 better than that between D4S451 and D4S2690); additional support for this location is provided by SCH analysis, which indicated that D4S451 and D4S2690 both map to region G, while D4S400 and D4S2691 map to region H (fig. 1). The BMP3 locus has equal support on either side of D4S2690; however, data derived from analysis of YACs encompassing BMP3 and D4S2690 has confirmed that BMP3 lies in the D4S451-D4S2690 interval (authors' unpublished observations). Additional support for the more proximal location of the BMP3 locus relative to D4S2690 was provided by the physical localization of BMP3 to region G, as determined by SCH analysis (fig. 1). Finally, the most likely location for the locus D4S2693 is distal to D4S2692 (lod 2 better than that between SPP1 and D4S2692).

All but one of the loci—i.e., D4S2693—showed significant evidence of linkage to DGI-II, as assessed by pairwise analysis (table 3). The strongest support for positive linkage was provided by SPP1, which yielded a pairwise Z_{max} of 11.39 at $\theta = 0$. D4S2690 also showed no recombination with DGI-II, but it was not completely informative in a number of critical meioses (table 4). The most likely position of the DGI-II locus within the fixed marker map, on the basis of linkage analysis in the CEPH pedigrees, is in the 6.6-cM interval between D4S2691 and D4S2692—$Z_{max} = 11.62$, as assessed by multipoint linkage analysis (fig. 3). The 1-lod support interval places DGI-II in a 3.2-cM interval around SPP1. The DGI-II locus could be excluded, with odds ≥1,000:1, from all other locations—with the exception of the D4S2690–D4S2691 interval, from which it could be excluded with odds of 12:1. Examination of the recombinant individuals revealed by pairwise linkage analysis (table 4) provides further support for the results of the multipoint analysis. However, tight double-recombination events were identified in three individuals, two of whom are affected while the third is unaffected. In all three cases an identical result was obtained when the genotypings of the relevant families were repeated on an independent DNA sample. Given that insoluble preparations of dentin matrix have been demonstrated to possess bone morphogenetic protein activity (Butler et al. 1977), the BMP3 gene was considered to be a candidate for the DGI-II locus; however, both the map position of the BMP3 locus and the identification of a recombination event between BMP3 and DGI-II in an affected individual (table 3) effectively exclude mutations in the BMP3 gene from a causative role in the pathogenesis of DGI-II.

Discussion

Previous segregation studies have shown that the DGI-II locus is linked to markers in the region 4q11-q21, and a number of candidate genes have been excluded from a causative role in the pathogenesis of the disorder (Ball et al. 1982; Crall et al. 1992; MacDougall et al. 1992). However, since all of the markers used in these studies have been RFLPs of relatively low informativity, the identification of flanking markers has not been possible. The primary aim of the current investigation was therefore to create a combined genetic and SCH map of highly informative STRPs around the DGI-II locus and to identify markers flanking the disorder. While the order of the loci predicted by the different mapping methods was consistent, linkage analysis in the CEPH pedigrees allowed only six of the STRPs to be positioned on the genetic map with odds ≥1,000:1. Nevertheless, both BMP3 and D4S400 could be ordered with respect to other markers, by combining the data generated by the two mapping methods with additional data from ongoing YAC contig assembly in the region. The combined results of the genetic and physical mapping therefore indicate that the most likely order of

Table 3

Pairwise Z Values for DGI-II

	Z AT θ =								
LOCUS	.00	.05	.10	.15	.20	.30	.40	Z_{max}[a]	θ
D4S2689	−29.55	3.48	3.96	3.88	3.55	2.51	1.18	3.97	.114
D4S451	−21.10	3.15	3.59	3.53	2.33	2.26	1.01	3.62	.113
BMP3	−.04	3.22	3.06	2.76	2.40	1.57	.66	3.22	.048
D4S2690	9.88	9.05	8.19	7.30	6.37	4.37	2.17	9.88	.001
D4S400	−.12	3.13	2.97	2.67	2.30	1.47	1.03	3.13	.048
D4S2691	5.01	8.54	8.12	7.43	6.58	4.58	2.25	8.56	.041
SPP1	11.39	10.43	9.44	8.39	7.29	4.95	2.38	11.39	.001
D4S2692	−5.54	4.89	4.81	4.45	3.95	2.72	1.30	4.92	.006
D4S2693	−.58	.73	.79	.73	.63	.38	.16	.79	.090

[a] At θ value shown in the rightmost column.

these loci is cen–D4S2689–D4S451–BMP3–D4S2690–D4S400–D4S2691–SPP1–D4S2692/D4S2693–tel.

Two of the markers on this map—D4S2690 and SPP1—show no recombination with DGI-II, despite the fact that they are located 8.0 cM from one another. Analysis of critical recombinants indicated that, although D4S2690 was not completely informative in a number of critical meioses, at least two tight double-recombination events must have occurred within one of the DGI-II families. Interestingly, a double-recombination event occurring between D4S2691 and D4S2692 was noted in CEPH family 1331, individual 11. While it is surprising that double-recombination events have occurred over such a small genetic distance, this region may be a recombination hotspot.

The most likely position for the DGI-II locus within the marker framework, as assessed by multipoint analysis, is in the 6.6-cM interval between D4S2691 and D4S2692. The confidence interval also places DGI-II within this region. The markers flanking the DGI-II locus—D4S2691 and D4S2692—have both been localized to region H via SCH analysis; physical mapping data therefore permit the localization of the DGI-II locus to be refined to the region 4q21-q23. Osteopontin, SPP1, which is synthesized by the dentin-forming odontoblasts (Butler 1989), lies within the DGI-II candidate region and shows no recombination with the DGI-II phenotype. However, a previous study has failed to reveal any disease-specific mutations in any of the six exons encompassing the coding sequence of this gene (Crosby et al. 1995). The data generated in the present study have also allowed us to exclude a second candidate gene, BMP3, from a causative role in the pathogenesis of DGI-II, on the basis of its map position and the observation of a recombination event in an affected individual.

The creation of a high-resolution genetic map around the DGI-II locus, together with the identification of flanking markers reported in the current study, will be

Table 4

Analysis of Individuals Showing Recombination between Chromosome 4q STRPs and the DGI-II Locus

	RESULT FOR LOCUS					
CLINICAL STATUS	D4S2689	D4S451	D4S2690	D4S2691	SPP1	D4S2692
Affected	R	NR	NR	...	NR	NR
Affected	R	NR	NR	NR	NR	...
Affected	R	R	NR	NR	NR	NR
Affected	NR	NR	NR	NR	NR	R
Affected	NR	R	...	R	NR	NR
Affected	R	R	...	NR	NR	R
Unaffected	NR	NR	...	R	NR	NR

NOTE.—R = recombinant individual; NR = nonrecombinant individual; and ellipsis (. . .) = uninformative or partially informative meiosis.

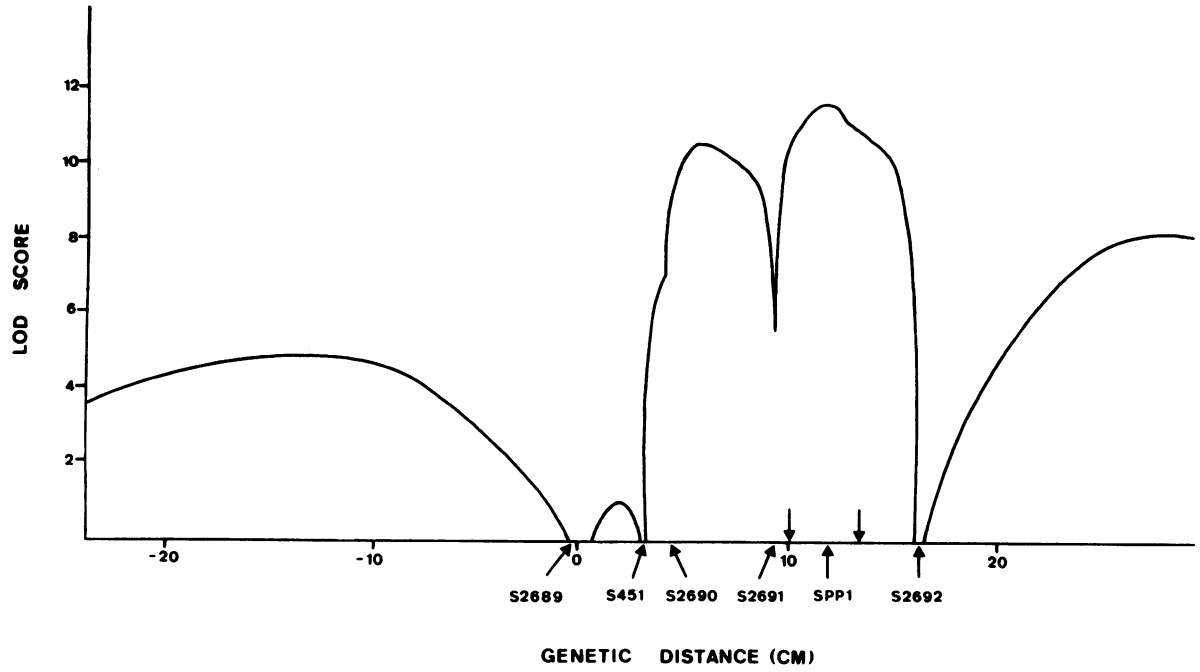

Figure 3 Multipoint map of chromosome 4q12-25 STRPs, calculated for DGI-II locus at various positions in a fixed marker map. Likelihood estimates are given in $\log_{10}$. The relative genetic position of D4S2689 has arbitrarily been placed at 0. The confidence interval (1-lod support interval), which spans a region of ~3.2 cM surrounding SPP1, is indicated by down-pointing arrows. The DGI-II locus is between D4S2691 and D4S2692 and probably is closer to the former.

central to the creation of a YAC contig across the DGI-II critical region. In this regard, the fact that SPP1 shows no recombination with the DGI-II phenotype will be an important adjunct to the cloning of the mutated gene, since it will provide an important anchor point for bidirectional walking toward the flanking markers.

In addition to the DGI-II locus, three other loci implicated in disorders of dental development have been mapped to this region of the genome. Extension, proximally and distally, of the combined genetic and physical maps documented in the current study should therefore prove useful in the further analysis of an autosomal dominant form of amelogenesis imperfecta (Forsman et al. 1994), juvenile periodontitis (Boughman et al. 1986), and Reiger syndrome (Murray et al. 1992).

Acknowledgments

We should like to thank the Human Genome Mapping Resource Centre, United Kingdom, for providing YAC clones. We thank the dentinogenesis imperfecta families for their cooperation, without which the present study would not have been possible. We should also like to thank Dr. M. Crall for clinical evaluation of the patients used in this study and also for preliminary analysis. The financial support of Wellcome Trust grants 034035/Z/91/Z and 042186/Z/94/Z and of NIH grants DE09170 and USPHS HG00835 is gratefully acknowledged.

References

Anand R, Riley JH, Butler R, Smith JC, Markham AF (1990) A 3.5 genome equivalent multi access YAC library: construction, characterisation, screening and storage. Nucleic Acids Res 18:1951–1956

Bakker E, Vossen RHAM, Riley BP, Sherrington R, Vergnaud G, Pearson NM (1994) The EUROGEM map of human chromosome 4. Eur J Hum Genet 2:210–211

Ball SP, Cook PJL, Mars M, Buckton KE (1982) Linkage between dentinogenesis imperfecta and Gc. Ann Hum Genet 46:35–40

Boughman JA, Halloran SL, Roulston D, Schwartz S, Suzuki JB, Weitkamp LR, Wenk RE, et al (1986) An autosomal dominant form of juvenile periodontitis: its localization to chromosome 4 and linkage to dentinogenesis imperfecta and Gc. J Cranio Genet Dev Biol 6:341–350

Buetow KH, Shiang R, Yang P, Nakamura Y, Lathrop GM, White R, Wasmuth JJ, et al (1991) A detailed multipoint map of human chromosome 4 provides evidence for linkage heterogeneity and position-specific recombination rates. Am J Hum Genet 48:911–925

Buetow KH, Weber JL, Ludwigsen S, Scherpbier-Heddema T, Duyk GM, Sheffield VC, Wang Z, et al (1994) Integrated human genome-wide maps constructed using the CEPH reference panel. Nat Genet 6:391–393

Butler WT (1989) The nature and significance of osteopontin. Connect Tissue Res 23:123–126

Butler WT, Mikulski A, Urist MR (1977) Noncollagenous proteins of a rat dentin matrix possessing bone morphogenetic activity. J Dent Res 56:228–232

Conneally PM, Edwards JH, Kidd KK, Lalouel JM, Morton NE, Ott J, White R (1985) Report of the Committee on Methods of Linkage Analysis and Reporting. Cytogenet Cell Genet 40:356–359

Crall MG, Schuler CF, Buetow KH, Murray JC (1992) Genetic marker study of dentinogenesis imperfecta. Proc Finn Dent Soc 88:285–293

Crosby AH, Edwards SJ, Murray JC, Dixon MJ (1995) Genomic organization of the human osteopontin gene: exclusion of the locus from a causative role in the pathogenesis of dentinogenesis imperfecta type II. Genomics 27:155–160

Dausset J, Cann H, Cohen D, Lathrop M, Lalouel J, White R (1990) Centre d'Etude du Polymorphisme Humain (CEPH): collaborative genetic mapping of the human genome. Genomics 6:575–577

Dixon MJ, Dixon J, Raskova D, Le Beau MM, Williamson R, Klinger K, Landes GM (1992) Genetic and physical mapping of the Treacher Collins syndrome locus: refinement of the localization to chromosome 5q32-33.2. Hum Mol Genet 1:249–253

Forsman K, Lind L, Backman B, Westermark E, Holmgren G (1994) Localization of a gene for autosomal dominant amelogenesis imperfecta (ADAI) to chromosome 4q. Hum Mol Genet 3:1621–1625

Goold RD, diSibio GL, Xu H, Lang DB, Dadgar J, Magrane GG, Dugaiczyk A, et al (1993) The development of sequence-tagged sites for human chromosome 4. Hum Mol Genet 2:1271–1288

Gyapay G, Morissette J, Vignal A, Dib C, Fizames C, Millasseau P, Marc S, et al (1994) The 1993–94 Genethon human genetic linkage map. Nat Genet 7:246–339

Lathrop GM, Lalouel JM, Julier C, Ott J (1984) Strategies for multilocus linkage analysis in humans. Proc Natl Acad Sci USA 81:3443–3446

——— (1985) Multilocus linkage analysis in humans: detection of linkage and estimation of recombination. Am J Hum Genet 37:482–498

MacDougall M, Zeichner-David M, Murray J, Crall M, Davis A, Slavkin H (1992) Dentin phosphoprotein gene locus is not associated with dentinogenesis imperfecta types II and III. Am J Hum Genet 50:190–194

Mills KA, Buetow KH, Xu Y, Weber JL, Altherr MR, Wasmuth JJ, Murray JC (1992) Genetic and physical maps of human chromosome 4 based on dinucleotide repeats. Genomics 14:209–219

Murray JC, Bennett SR, Kwitek AE, Small KW, Schinzel KW, Alward A, Weber JL, et al (1992) Linkage of Reiger syndrome to the region of the epidermal growth factor gene on chromosome 4. Nat Genet 2:46–49

Tabas JA, Zasloff M, Wasmuth JJ, Emanuel BS, Altherr MR, McPherson JD, Wozney JM, et al (1991) Bone morphogenetic protein: chromosomal localization of human genes for BMP1, BMP2A, and BMP3. Genomics 9:283–289

Wijmenga C, Dauwerse HG, Padberg GW, Meyer N, Murray JC, Mills K, van Ommen G-JB, et al. FISH mapping of 250 cosmid and 26 YAC clones to chromosome 4 with special emphasis on the FSHD region at 4q35. Muscle Nerve (in press)

Witkop CJ (1957) Hereditary defects in enamel and dentin. Acta Genet 7:236–239